Embedded optical fibres for monitoring pressurization and impact of filament wound cylinders

Erik Sæter[a]*, Kaspar Lasn[a], Fabien Nony[b] and Andreas T. Echtermeyer[a]

[a] *Department of Mechanical and Industrial Engineering, Norwegian University of Science and Technology (NTNU), Richard Birkelands vei 2B, 7491 Trondheim, Norway*
[b] *Polymer Synthesis & Processing Lab., CEA/ Le Ripault – Materials Dept.*
Corresponding author: erik.sater@ntnu.no

ABSTRACT

Filament wound composite pressure vessels have found use throughout many industries for storing high-pressure gases. The ability to investigate the vessels for possible damage from accidental impact loads is important for applications in the transport sector. Standard non-destructive methods are complicated. This paper describes a method to permanently monitor pressure vessels for their structural integrity.

The method is based on standard telecommunications grade optical fibres embedded in the composite overwrap as a network of distributed strain sensors. Challenges regarding the practical implementation of optical fibres, and post-processing of signals, are discussed. During pressurization, the optical fibres were used to measure strains in several thicknesses of the composite layup. The cylinders were impacted and the backscattered light from optical fibres was then analysed to visualize the position and the severity of damage. The interrogation of embedded optical fibre networks is successfully demonstrated as a promising method for structural health monitoring of composite pressure vessels.

Keywords: Pressure vessel, COPV, optical fibre, OBR, Rayleigh backscatter, structural health

INTRODUCTION

Composite overwrapped pressure vessels (COPVs) are gaining momentum in commercial applications as high-pressure gas containers. Their high strength to weight ratio enables transporting higher payloads than traditional metallic cylinders. When the COPVs are used on trucks or in other exposed applications health monitoring is important to ensure that impact from accidental external loads has not created any significant damage.

The standard approach for detecting damage is the use of non-destructive evaluation (NDE) methods, such as visual inspection, acoustic emission, ultrasonic testing, radiography, thermography etc. [1]. These methods often require special loading or handling conditions during inspection and are therefore only suitable for periodic inspections rather than for continuous monitoring. Furthermore, the non-destructive detection of fibre failures, which are usually accompanied by large delaminations, has been recognized as a bottleneck in the evaluation of residual performance of pressure vessels [2]. It is worth pointing out that fibre failure is the main mechanism leading to failure of a composite pressure vessel. An improved approach for detecting damage is to employ structural health monitoring systems for direct feedback from the composite structure allowing determining whether an impact has occurred and where it is located. Such a system based on a network of optical fibre strain measurements is addressed in the current study.

Approaches where an integrated sensor network is embedded into composite cylinders have gained popularity over past decades [3]. Optical fibres (OF) can be employed as a real-time *in situ* structural health monitoring (SHM) system throughout manufacturing, transport, installation, and the service life of the pressure vessel.

In recent years, experience has been built up by using Fibre Bragg Grating (FBG) optical fibre sensors [4–12] and long gage interferometric optical fibre sensors [13–17] for SHM of COPVs. A detailed description has been presented how the temperature and strain changes were monitored from the manufacturing stage to in-service behaviour for externally pressurized filament wound structures [18–20]. Earlier approaches have also looked into intensity sensors based on optical signal attenuation [21–23]. Aforementioned fibre optic sensors are based on either long gage lengths, which average the signal response over the whole structure; or they are essentially point sensors, where only a limited number of structural locations is interrogated. None of these fibre optic solutions provides high-resolution full field strain measurements over the entire pressure vessel structure.

Current work employs a novel distributed strain sensing system utilizing optical backscatter reflectometry (OBR) on the principle of Rayleigh backscattering [24–26]. The OBR technology makes it possible to measure strains with millimetre-range spatial resolution, over relatively long distances (ca. 70 m), using a regular telecommunications optical fibre. This fine spatial resolution is currently unparalleled by other distributed sensing methods (Brillouin or Raman backscattering). The OBR with Rayleigh backscattering opens new possibilities for embedding high-resolution sensor networks into the composite, covering the entire structure, and thereby providing a full-field measurement of strains or temperatures. First implementations of the OBR technology for COPV monitoring have been reported by Maurin *et al.* [27], and by the manufacturer of the OBR interrogator system, with Klute *et al.* [28].

Current work is carried out to validate the OBR inspection methodology for composite pressure vessels. The following study demonstrates how the embedded network of optical fibres can be used to obtain high-resolution strain measurements covering the entire cylindrical surface of the structure. Challenges regarding the practical implementation (embedding) of optical fibres, and post-processing of data, are discussed. It is concluded that a network of OFs (either embedded or surface mounted) is both a practicable and a promising method for SHM of COPVs.

DISTRIBUTED FIBRE OPTIC SENSING BY OBR

This section gives a short introduction to distributed sensing technology based on Rayleigh backscattering (OBR). For a better overview of the whole field of distributed fibre optic sensing, two recent reviews can be consulted [29,30]. For this work, the OBR apparatus and its accompanying software were purchased from Luna Innovations [31].

As optical fibres are embedded into the composite, or mounted on the surface, any perturbations in the host composite (such as deformations or temperature changes) affect the optical signals propagating in the fibre. OBR reveals the temperature or strain change from any point along the optical fibre by using light scattering – interaction between the light and the fibre. The scattering does not alter the properties of the fibre, and arises from non-homogeneities such as variations in refractive index, density, composition or structure of the optical fibre. These variations are considered as random and non-propagating over the life of a fibre, often called a characteristic fingerprint for one specific fibre. Measurements have shown that the

characteristic pattern of the fibre does indeed remain repeatable and unique over several years [32].

The reflectometer sends a signal from a swept-tuneable laser, and by increasing the frequency scanning range, the spatial resolutions of measurements can be lowered to 1 mm or less. For example, Pedrazzani *et al*. [33] report measurements with 0.5 mm resolution in a composite coupon. The sensing length is limited to tens of meters (ca. 70 m), but it can be extended at the expense of coarser spatial resolutions, up to 2 km.

As strain is applied to the fibre, it stretches the characteristic variations, which translate into a shift in the spectral content of the backscatter signal. In the analysis of the signal the fibre is divided into many short sequential sections (which define the gauge length) along the entire length of the fibre. The spectral content of each section is compared between the measurement state and a previously measured reference state. The cross-correlated spectral shift between these two states is converted to strain by an empirical calibration coefficient. This process is repeated along the fibre length, forming a distributed measurement with selectable gauge length and sensor spacing variables. Both the gauge length and sensor spacing are chosen during post-processing, and the measured signal can simply be re-analysed unlimited times to find the best combination for these two input variables. The same applies in case of updates in the software.

The noise in the strain measurements is low, typically below ±5 microstrain and comparisons to electrical strain gauges give very good agreement, with mean differences reported to 5 % or less [33,34]. The OBR measurement takes a few seconds to perform, and this limits the technology currently to quasi-static measurements.

MATERIALS AND METHODS

Pressure vessels

The pressure vessels for this study were made by filament winding around a hybrid mandrel, consisting of steel domes and a cylindrical polyethylene mandrel. The dimensions of the cylinders are as follows: cylindrical section length 600 mm, mandrel diameter of 140 mm and ca. 3 mm thick composite overwrap. Slightly different dome geometries were used throughout the project, which is expected to have no effect for the current study. To ensure pressure tightness, a thin polyurethane liner was injected after the filament winding was finished. Examples of typical pressure vessels before and after burst testing can be seen in Figure 1.

Figure 1: Pressure vessels before and after burst testing.

The structural fibres of the pressure vessel overwrap are all carbon, type Grafil 34-700 24k by Mitsubishi Rayon. The epoxy resin is from Hexion, mixed from two components: EPIKOTE MGS RIMR 135 and EPIKURE curing Agent MGS RIMH 137. The layup for the composite overwrap is $[90°_2 / (\pm15°)_2 / 90°_2]$.

The filament winding was carried out on a MIKROSAM automated machine and the winding parameters are briefly summarized below.

- **Pre-tension**: was kept constant at 40 N for all windings, both for hoop and helical layers.
- **Bandwidth**: the same carbon fibre filament was used for all vessels with a bandwidth of 5 mm. Only one roving was used in the winding process.
- **Winding speed**: determines the rate at which the filament runs through the system. The speed was usually set as high as possible without giving excessive spilling/splatter from the resin bath.
- **Hoop winding**: the pitch is determined by the bandwidth.
- **Helical winding**: have the same angle of $\pm15°$ throughout all vessels in the study. Each winding pattern has a given number of cycles, which determines how much physical fibre material (or number of filament windings) is put onto the mandrel. This varied slightly between vessels and is specified later in Table 1.
- **The amount of resin**: was controlled by a scraper system, to make sure the filaments were completely wetted. During winding, the excess resin was removed from the vessel surface, to ensure a high fibre volume ratio.

Instrumentation: optical fibres and strain gauges

Standard telecommunication grade optical fibres were employed for embedding and strain measurements. The diameters of the fibre core, cladding and coating were 6.5 μm, 125 μm and 155 μm, respectively. These fibres were chosen based on previous good experience [35,36].

The measuring fibre, denoted as primary coated optical fibre (PCOF), was embedded into the composite layup. The PCOF was spliced to a more robust secondary coated optical fibre (SCOF), which transferred the signal after egressing to the outside of the vessel. SCOF also includes a connector port to the LUNA OBR 4600 apparatus. An overview of the OF sensor and the interrogator is shown in Figure 2. Even though optical fibres were only embedded inside the layup for this study, surface mounted optical fibres can also be used for impact detection and strain monitoring. One concern related to surface mounted OFs is the lack of natural protection from the composite layup.
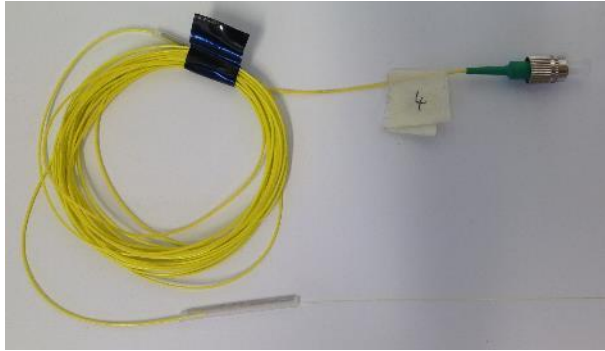
*(a) The sensor: SCOF with a connector and a tag, spliced to PCOF*   *(b) The interrogator apparatus, LUNA OBR 4600*

Figure 2: The sensor and the interrogator for distributed strain measurements

The difficulties of handling fragile optical fibres are well known. Davidson and Roberts [37] give a good overview of methods of optical fibre ingress and egress from the composite, and possible ply defects due to embedding of OFs. In order to embed the OFs into the vessel layup, the filament winding process was put on hold. The optical fibres were then wound between pairs of hoop carbon fibre layers. The first set of optical fibres (first intralayer) is positioned one hoop layer out from the mandrel, and the second set of fibres (second intralayer) is positioned one layer in from the outer surface (see Table 1).

For filament wound structures, the OF placement will usually not be exactly parallel to the composite reinforcement fibres. This is due to the larger pitch distance of OFs, usually 20 mm or 30 mm to minimize the OF consumption, compared to the 5 mm pitch of hoop reinforcements. For current mandrel, the pitch angle of OFs therefore varies between ca. 2.6° and 3.9°, whereas the pitch angle of fibre filaments is 0.65°. Some resin rich regions surrounding the optical fibre will therefore always be present due to the mismatch of these angles. However, the difference of pitch angles is small causing only minor disruption to the surrounding laminate, and the composite properties are expected to be little affected. The micrographs of embedded optical fibres (e.g. Figure 3) show minimal disturbance (resin pockets and voids) surrounding the individual optical fibres, not much as compared to the overall laminate. There could also be issues with micro-bending of OFs between the reinforcing fibres, as discussed in the later section describing the Running Reference Method. These possible microbending effects, while important to take note, are considered out of scope for current analysis.
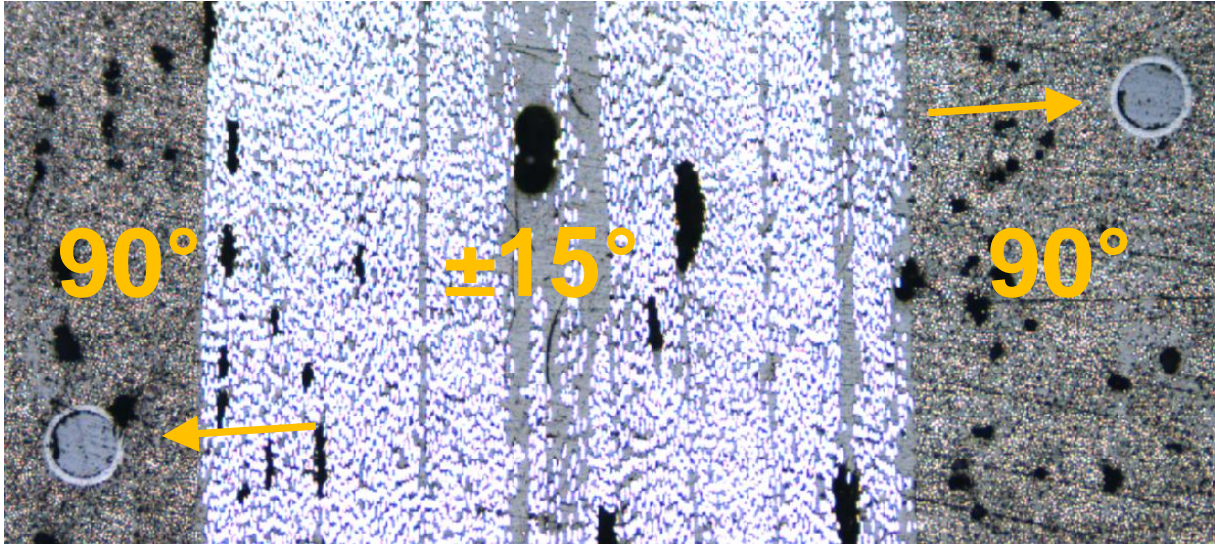
Figure 3: Optical fibres embedded between the hoop layers of filament wound pressure vessels. Arrows point to the optical fibres at two depths in the composite overwrap.

Two different optical fibre configurations were utilized, as shown in Figure 4. The first, an impact grid, consists of one optical fibre forming two sub-grids inside a 3 x 3 cm^2 region. The fibre is guided through two concentric squares with 1 x 1 cm^2 and 3 x 3 cm^2 sizes. The grid positioning with reference locations is shown in Figure 4(a) and snapshots of the actual embedding of grid OFs in Figure 5. The second main fibre configuration is called a hoop placement where the optical fibre is laid down on a spiral pattern, with a pitch of either 20 or 30 mm. The hoop optical fibre configuration is also shown in Figure 4(a) and Figure 5. The number of embedded optical fibres differs between the pressure vessels, as reported in Table 1. For vessels 1 to 3, there was one impact grid and three hoop optical fibres for both intralayers. This configuration is shown in Figure 4(a). The hoop fibres had a pitch of 30 mm and offsets of 10 mm relative to each other, meaning that the fibres cover the entire cylindrical section with a spacing of 10 mm. In vessels 8 to 10 there were no impact grids, only two hoop fibres in both intralayers. The hoop fibres for these vessels had a pitch of 20 mm and an offset of 10 mm to get the same 10 mm spacing as for the first vessels. Using several independent fibres to cover the cylinder surface increases the survival yield for optical fibres, considering production and the impact event. The length of the OFs inside the vessel, from reference to reference, was approximately 9 m for Vessels 1 to 3, and approximately 13.5 m for Vessels 8 to 10.
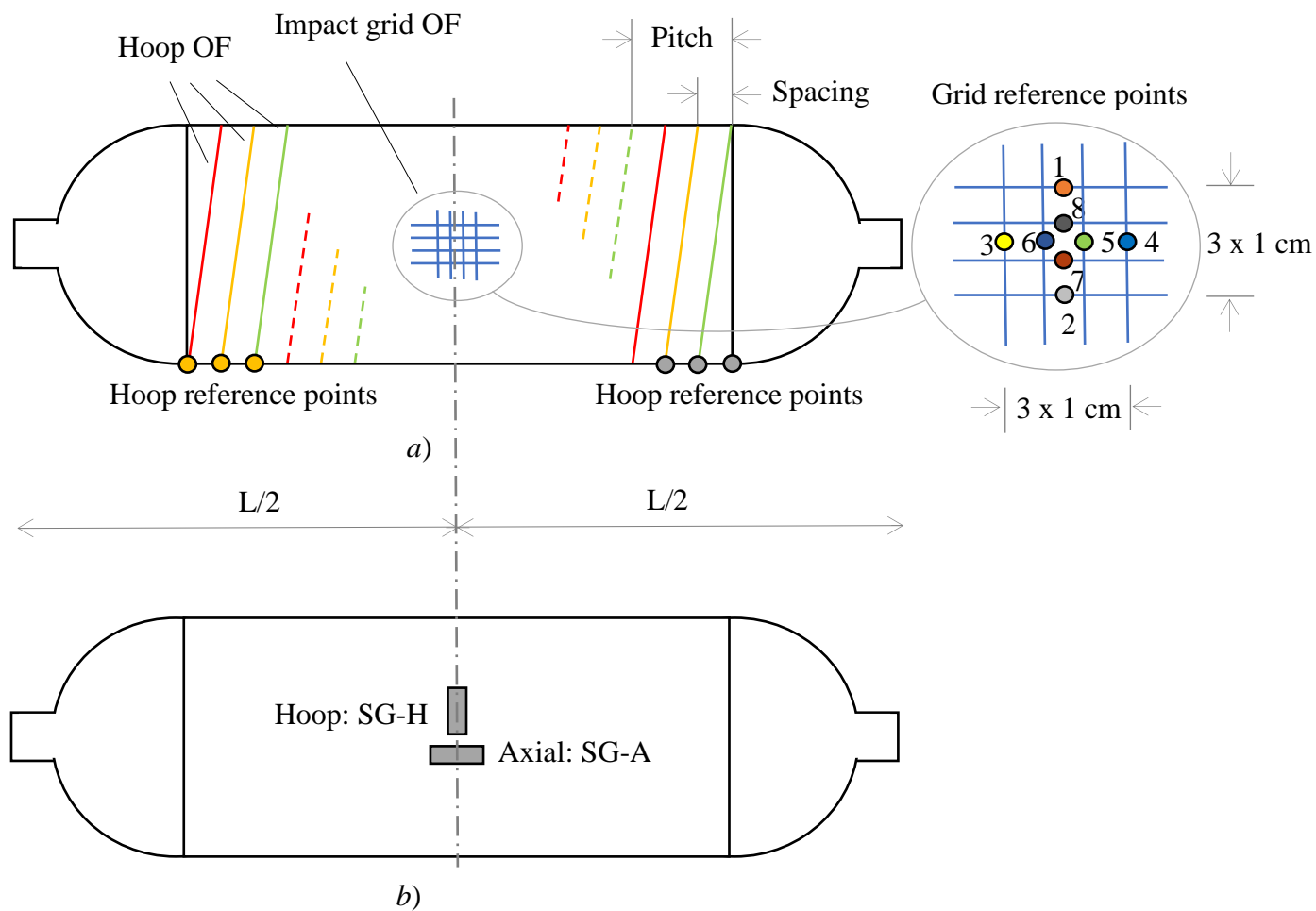
Figure 4: The pressure vessel instrumentation: a) OF positions and reference point locations b) SG positions

The OBR scans provide longitudinal strain values as a function of position along the optical fibre. In order to map the position of the strain signal to the actual position on the vessel, reference positions were established, as seen in Figure 4(a). This was done by applying a small force directly on an OF after it had been placed on the vessel, and simultaneously running a scan to record the spatial position of the signal. The referencing was carried out in the middle of the filament winding process. Both start and ending points for the optical hoop fibres were recorded. For the impact grids, the reference positions were recorded at the midpoints of both concentric squares. After the fibres were positioned on the vessel, and the reference positions established, the winding was continued. The SCOFs were secured to the vessel after the layup was completed, as seen in Figure 5.
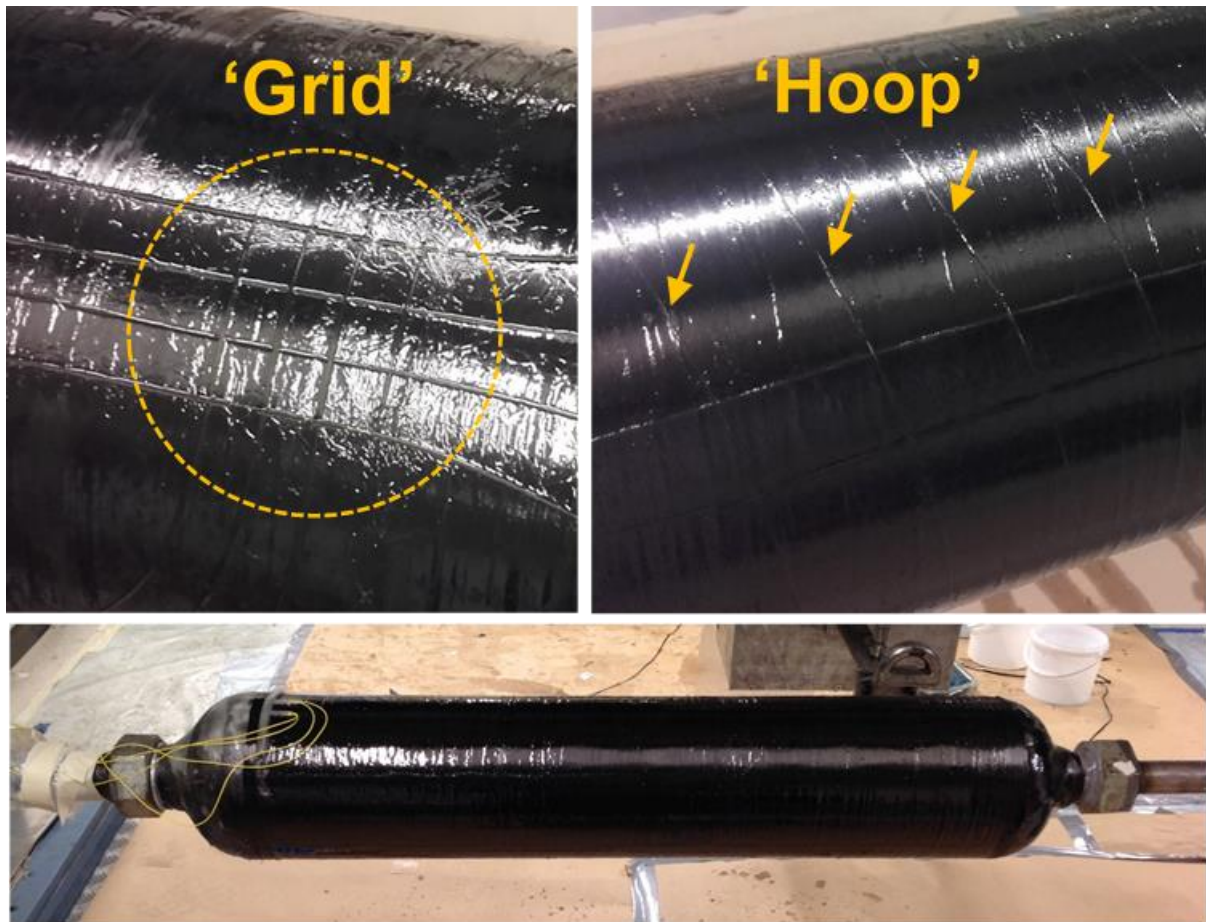
Figure 5: Placement of embedded OFs during manufacturing and a finished pressure vessel.

The first batch of pressure vessels had a low OF survival rate (ca. 50 %). Most of the fibres failed at the point where they egressed from the laminate, at the neck of the pressure vessel. The neck was connected to the fixture of the winding machine with a large nut. The fibres egressed from the composite in the neck region and got damaged when the nut was unwound after filament winding. The solution was to put a shim between the nut and the composite, as seen in Figure 6. In addition, when the winding was finished, a thin layer of glass fibre was laid over the dome to protect the entire egress region (Figures 5 and 6). The shim was covered with a thin layer of resin, to prevent it from moving when the nut was removed. By utilizing this technique, the survival rate of the OFs increased from approximately 50 % to almost 100 %.
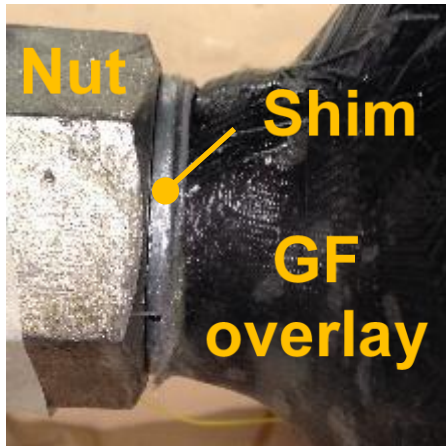
Figure 6: Protective shim at the neck

In addition to embedded OFs, surface mounted strain gauges (SGs) were used for monitoring the vessels during pressurization. The SGs by Tokyo Sokki Kenkyujo, types FLA-5-11-1L and FLA-6-11-3L, had 6 mm and 5 mm gauge lengths, respectively. Both axial and hoop SGs were mounted in the centre of the cylinder, as shown in Figure 4(b).

Impact and burst testing

The experimental tests were split in two parts: impact testing and burst testing. The OBR measurement process requires a quasi-static behaviour of the measured object, which meant that pressurization was put on hold when the OBR scans were performed. The pause in pressurization would last for approximately 30 s. Measurements were carried out at the following pressure levels: 10, 20, 30, …, 100, 120, 140, …, 200, 250, 300 [bar]. The pressurization rate was approximately 0.7 bar/s.

The impact itself and post-impact inspection with optical fibres were performed on non-pressurized vessels. The impacts were carried out using a drop tower assembly. The impact setup, shown in Figure 7, consists of a jig, a guide tower and a steel $\emptyset = 20$ mm hemispherical impactor. The jig had foam padding on vertically supported sides. The vessel was lightly clamped between two vertical profiles, along the cylindrical length. Impacts were usually performed before the burst tests. Only in the cases when healthy pressure vessels were leaking, the impact testing was performed post-pressurization to gather more data from optical fibre networks. All of the pressure vessels and impacts presented in this study are summarized in Table 1.
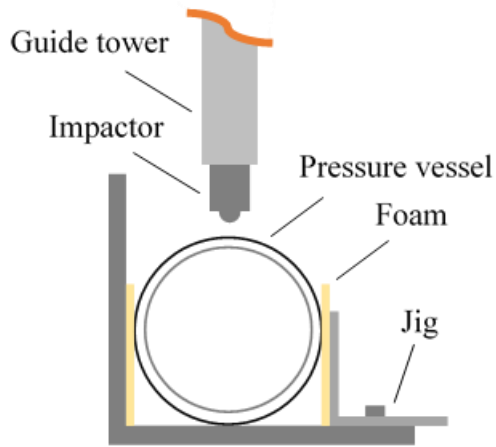
Figure 7: The impact setup

Table 1: Summary of pressure vessels, embedded optical fibres and impacts

Vessel	Layup	# cycles in helical	Impact energy [J], number in (…) after pressurization	Hoop OFs	Grid OFs
1		87	N/A	3 + 3	1 + 1
2	90/**OFs**/90/	89	60	3 + 3	1 + 1
3	±15 /±15/	89	30	3 + 3	1 + 1
8	90/**OFs**/90	89	60, (40, 20)	2 + 2	0
9		89	(60, 40, 20)	2 + 2	0
10		89	(100)	2 + 2	0

VALIDATION OF OPTICAL FIBRE STRAIN MEASUREMENTS

Before proceeding with impact damage detection, the optical fibre measurements were validated by comparing strains to a standard method – electrical strain gauges mounted on the surface. Strains from several optical fibres were also compared to each other to measure dispersion between similar measurements.

The LUNA desktop software gives the user the possibility to choose resolution parameters for distributed strain sensing. Recorded optical signals can be post-processed to distributed strains based on two resolution parameters – sensor spacing and gauge length. Table 2 shows three chosen resolution modes for the analyses, based on previous experience with measuring composites. Mode 1 corresponds to a very fine spatial resolution. It can be described as 5 mm length virtual strain gauges, placed with 1 mm spacing next to each other. The gauge lengths of virtual sensors in Mode 1 are the same as in physical strain gauges in this work, however the placement of these virtual sensors has a lot of overlap, with only a 1 mm step. Mode 3 describes much coarser spatial resolution – virtual strain gauges with 30 mm length, placed with 10 mm spacing. Fine spatial resolutions (such as Mode 1) introduce local fluctuations into the measurements. These fluctuations are increasingly averaged out with coarser parameter configurations such as Mode 2 or Mode 3. For healthy cylinders, the strain field around the

cylinder midpoint is close to uniform and a high spatial resolution is not necessary, meaning that mode 3 was used almost exclusively when no impacts were involved.

Table 1: The resolution parameters for OF strain analysis

Mode	Sensor spacing	Gauge length
1	1 mm	5 mm
2	5 mm	10 mm
3	10 mm	30 mm

Since the embedded OFs measure strains over the whole cylindrical section, only a segment of the fibre was used to compare it to the SGs. As mentioned in relation to Figure 4, the optical fibre inside the vessels had a length of 9 m on Vessels 1 and 2, and 13.5 m on Vessels 8 to 10. By averaging the OF strains over a 5 m section at the centre of the cylinder, a mean OF strain value was obtained. The reference scans for OFs were recorded after the manufacturing process was completed, i.e. the reference state that is considered with zero strains may actually have residual strains from the manufacturing process. The strain gauges were also glued on the surface after the manufacturing was completed, and therefore have the same zero reference state. The reference state, which remains the same, is compared to new scans made at successive pressure levels, in the following analysis. All of the measurements were carried out at constant room temperature. The comparison plots are seen in Figure 8 and 9. The plotted data is named after the following convention: the first part refers to the pressure vessel number, and the second part refers to strain gauge (SG), inner (I) or outer (O) intralayer, and fibre number, or the fibre grid (G).
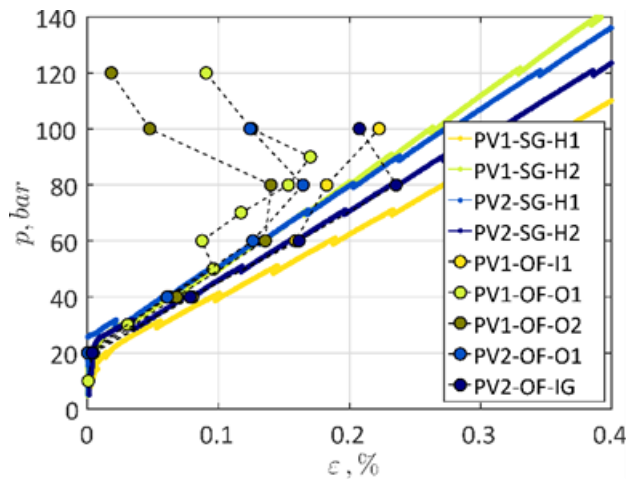

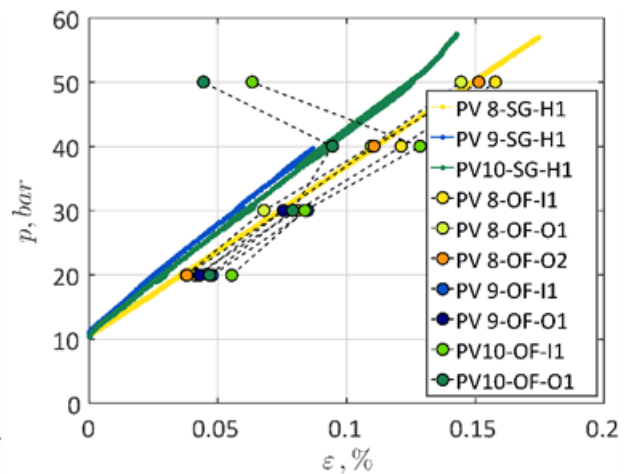Figure 8: Pressure vs strain in pressure vessels 1 and 2 (Mode 3).

Figure 9: Pressure vs strain in vessels 8, 9, and 10 (Mode 3). Kept separate from 1 and 2 due to vessels failing burst test and reaching low max.

During pressurization up to 50 bar, a good correlation between SGs and OF strains was observed. However, the hoop OFs struggled to give meaningful results when the pressure exceeded 50-60 bar, as seen in Figure 8. The strains in the OF grid agreed with the strain gauges

all the way up to 80 bar. For the OF grid, the averaged section was only 30 mm long due to the physical size of the grid. At first take, ca. 50-60 bar appears to be the measurement limit for hoop OFs embedded in these cylinders. This pressure corresponds to the first onset of matrix cracks in the composite overwrap. The issue of failing OF measurements, already at low

pressures, is further discussed in the upcoming sections. Although the analysis is struggling above 50 bar, some observations were made below this pressure level. The OF strains from the inner and outer intralayers show very similar behaviour, and the strain gradient agrees with the SGs mounted on the surface. This is expected due to a thin composite shell. The hoop OF strains from the five different cylinders are also in agreement. Even though there initially were noise issues above 50-60 bar of pressure, the raw signals in most of the OFs of Vessels 1 and 2 were recorded all the way up to burst pressure.

RUNNING REFERENCE METHOD

As observed in the previous section, the strain readings at internal pressures above 50-60 bar are suffering from noise. Faulty splices or bad connectors are two usual suspects. The geometric constraints in the fibre egress area can also lead to excessive curvature of the secondary coated or primary coated optical fibre. As seen from impacts, damages around the optical fibres can lead to disturbances in the signal. This also includes possible voids around the OFs (see Figure 3). Furthermore, the embedded optical fibres can experience situations similar to micro-bending [25,30]. In this case, the optical fibre micro-bends in between two fibre layers, similar to being compressed between two corrugated surfaces, resulting in the attenuation of the output. The noise level increases when the fibre is embedded between plies with a different orientation. Last but not least, the noise issue could be post-processing related. The software uses a correlation function to calculate strains between two states – measurement state and the reference state. If the change in temperature or strain between two measured states becomes larger than the correlation peak width (wavelength shift is larger than the wavelength peak itself), the analysis will give zero correlation [29].

During the validation measurements (OF comparison to other OFs and strain gauges), the noise in the strain readings appeared when the pressure exceeded ca. 50 bar. At this pressure level matrix cracks started to appear, and due to the OFs not being exactly parallel with the carbon fibres, the matrix cracks would occasionally cross the OFs at some locations. These matrix cracks will cause high local strains, which disrupt the signal. The OFs were obviously no longer able to track the increasing strains when the pressure reached 100 bar, as seen in Figures 10 and 11. This manifested as measuring falling average strains, due to outliers, even though in reality the strains were increasing. An increasing number of data points drop out of the average region, which drags down the average strains. Above 100 bar, the strain results mostly displayed noise, rendering the OFs useless for strain analysis. As previously mentioned, the grid fibres were able to give realistic strain readings at slightly higher pressures compared to hoop OFs. Grid fibres travel in the axial direction to the centre of the vessel, and proceed to run through several loops there, meaning that they were likely crossing many more matrix cracks along the way.

Altogether, we cannot conclude what was the reason causing the attenuation and the noise in the signal for pressures over 50-60 bar. Many causes are possible, as discussed earlier. However, in the following we present a remedy that effectively mitigates this issue.
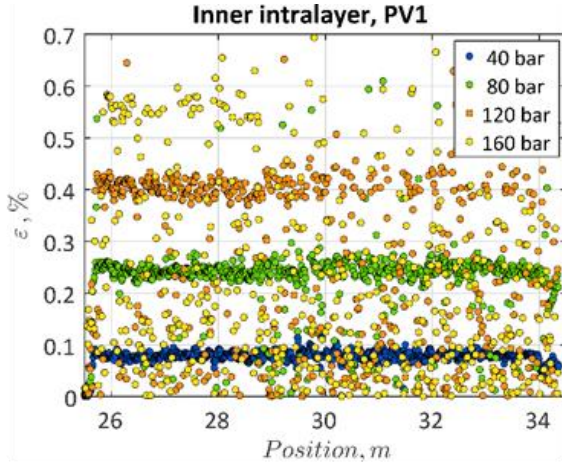
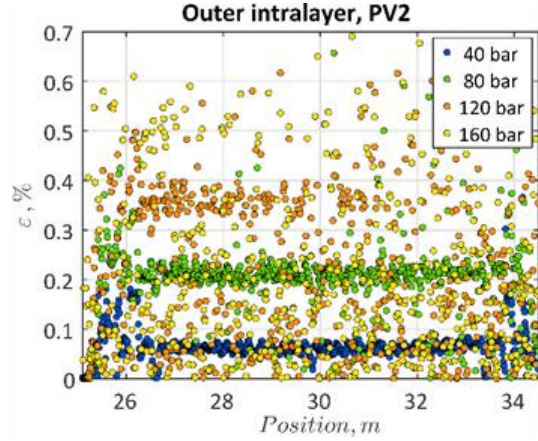Figure 10: Noise problems above 100 bar in Vessel 1 (Mode 3)

Figure 11: Noise problems above 100 bar in Vessel 2 (Mode 3)

In order to improve the results from the OF strain analysis, a new approach to evaluate the strains was suggested. In previous analyses, the reference was kept constant and the measurements at each new pressure level were compared to the original empty cylinder reference, to determine strains at the new level. The new method is based on using a running reference, similar to work reported by Maurin *et al*. [27], and Heinze and Echtermeyer[38], summing up all the individual strain changes to reach the strain at the desired pressure level. The algorithm for running reference can be summed up in Equation (1):

$$\Delta\varepsilon_{P_0 \to P_n}(s) = \sum_{i=1}^{i=n} \Delta\varepsilon_{P_{i-1} \to P_i}(s), \tag{1}$$

where $\Delta\varepsilon_{P_0 \to P_n}(s)$ is the strain increase from a base pressure level P_0 to a given pressure level P_n in position s along the optical fibre, and $\Delta\varepsilon_{P_{i-1} \to P_i}(s)$ is the change in strain between the intermediate pressure levels at position s. Successful results of implementing the algorithm can be seen in Figures 12 and 13. Compared to the constant reference, the running reference of Eq. (1) provides realistic strain measurements to very high pressure values, and gives comparable results to the strain gauges. The difference between the two post-processing methods is clear when comparing Figure 8 to Figure 12. With the running reference method the OFs follow the SGs almost all the way to 300 bar, approximately 90% of the burst pressure for Vessel 1 and 2. Vessel 2 was subjected to an impact before pressurization, and the repercussions of this become visible at elevated pressures, which is also seen in Figure 13. At 160 bar the fibre appears to be cut off at the middle of the cylinder, which is where the impactor struck. When comparing Figure 13 to the constant ref. method for the same cylinder in Figure 11, the signal has less noise.
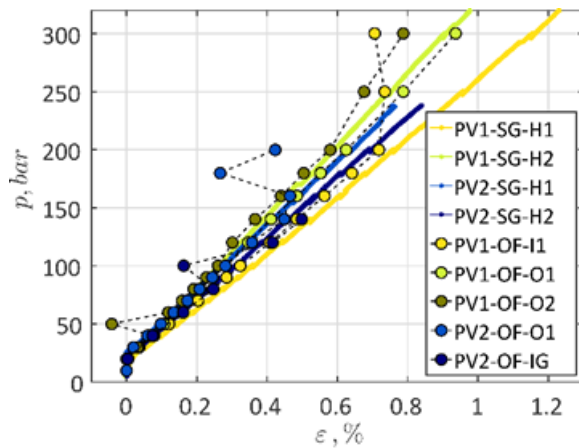
Figure 12: Pressure vs strains in Vessel 1 and 2, running ref. method (Mode 3)
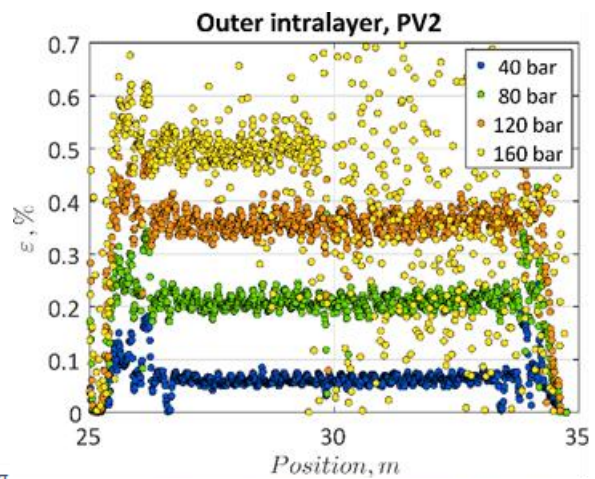

Figure 13: Strains vs position in Vessel 2, running ref. method (Mode 3)

The running reference method clearly improves strain readings at higher pressures, however, there are still signs of noise when measuring strains close to burst pressure levels, or measuring around a damaged area. The presence of noise can in those cases be interpreted as signs of damage, and highlights the presence of matrix cracks or other causes for localized abrupt strains. Noise may also be caused by overly large steps for strain measurements taken at higher pressures (50 bar steps for pressures exceeding 200 bar), which increases the possibility for zero correlation between the calculated and reference states, as discussed earlier.

IMPACT DETECTION AND VISUALIZATION

The embedded optical fibres do not only have a purpose of monitoring strains. More importantly, they serve as a Structural Health Monitoring (SHM) system. The possibilities of the OBR enable to use OFs for detecting strains with a very high spatial resolution.

Failing optical hoop fibre – unpressurized
The simplest impact detection method is based on the fibre's ability to transfer a signal. A damage large enough to sever or significantly damage the fibre is an indicator of damage to the vessel. Figure 14 shows how the amplitude peak from the end of the fibre shifts to the location where the fibre is severed by the impact. Similar experiments have been carried out by others before, e.g. Knapp and Robertson [21], however the properties of the OBR enable also to determine the location of the fracture. Both hoop and grid OFs successfully detected impacts in this way. The hoop method does not rely on knowing where the impact will take place, as the whole cylindrical region is covered by a grid of OFs. For the vessel presented in Figure 14 the severed fibre pinpoints the location of impact for a hoop optical fibre. This vessel had already been impacted and severed at a previous occasion, thus only the section of fibre between 24.2 and 28.8 m, was transmitting signal during this final impact. Typically, the optical fibres in the outer layer became severed. Impact energies varied from 20 J to 100 J, and none were able to sever fibres in the inner intralayer. On the other hand, even the lowest energy impacts could sever optical fibres in the outer layer, positioned one hoop layer deep from the surface. This finding supports the idea of embedding the sensor inside the composite, which differs from most other NDE methods[1].
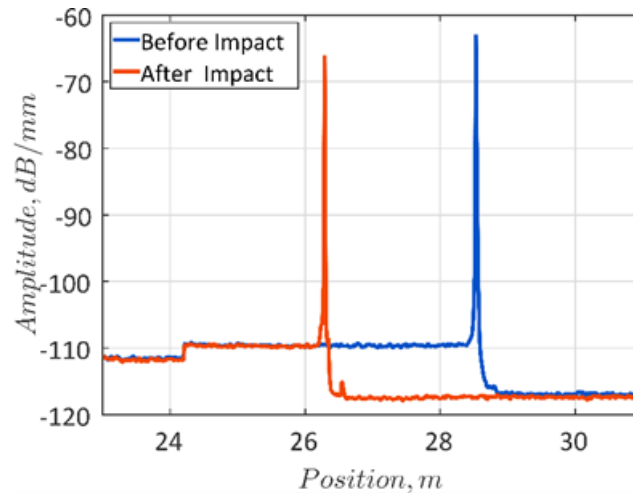
Figure 14: Hoop fibre signal in Vessel 8 before and after the 20 J impact. The OF is inside the vessel between 24.2 m and 28.8 m locations, in the outer intralayer.

Measuring strains due to impact

The full potential of the OBR becomes more apparent with the use of strain analysis. The strain sensing is based on comparing pre- and post-impact measurements, or investigating the changes in the strain field during pressurization. For all impact cases Mode 2 parameters were used, to keep the strain sensing resolution as high as possible without excessive noise. From measurements during the production, it was observed that the OFs detect residual strains. An impact energy high enough to cause a sufficient damage of the composite will lead to a release of these residual strains and possible inelastic deformations. This change of strain can be measured when the vessel is not pressurized. When the vessel is pressurized, strain concentrations caused by the impact damage can also be detected.
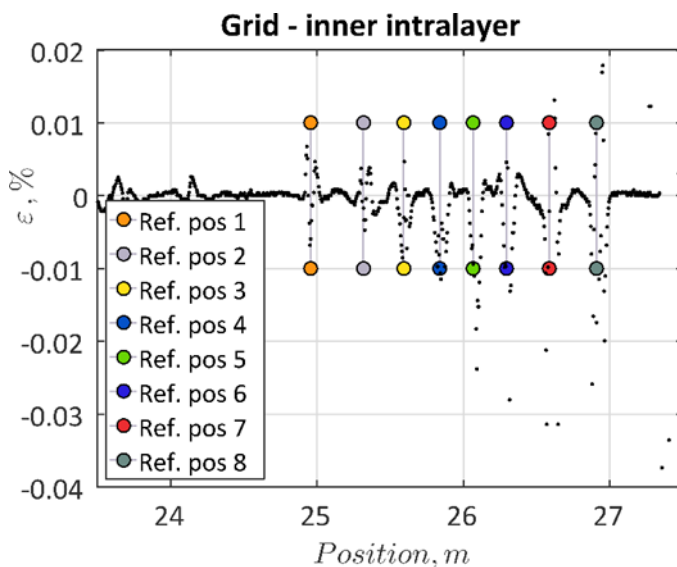

Figure 15: Strains vs reference markers in the grid, Vessel 1 (Mode 2)

Strains in fibre grids – unpressurized

When analysing an impact with the OF grid (see Figure 4), the impact location was positioned to the centre of the grid, made up of two concentric squares. The strain readings from a 60 J impact are shown in Figure 15. Points 1 to 4, the midpoints of the larger square, register much lower absolute strain values than points 5 to 8, the midpoints of the smaller square (see Figure

4a). The smaller square is physically closer to the impact location. This way, the extent of the damage can be tracked accurately in two directions. However, as a detector, the grid configuration requires much manual labour when placing the fibres into the pressure vessel and would not be practicable in a real structure. In addition, impact can only be detected within the grid. However, the location of accidental impacts is typically not known for gas containers and may happen outside the grid. Putting many grids on the pressure vessel would resolve this issue, but is not practical.

Strains in optical hoop fibres - unpressurized
Much information can be obtained by looking just at hoop strains, and a long sequence of hoop fibres is easily installed on the vessel. A comparison of hoop fibre strain measurements can be seen in Figures 16 and 17, which highlights the difference in the residual strains in inner and outer intralayers. The continuous peaks forming around the impact location depend on the value of the residual strain being released, which should be the same if caused by a large or a small impact. However, the higher energy impacts appear to have higher strain peaks around the impact location, as well as more scatter in strain values, which extend higher than the continuous peak. The difference between the two intralayers (Figures 16 and 17), confirms that the location – depth of the OFs – is also relevant for impact detection.
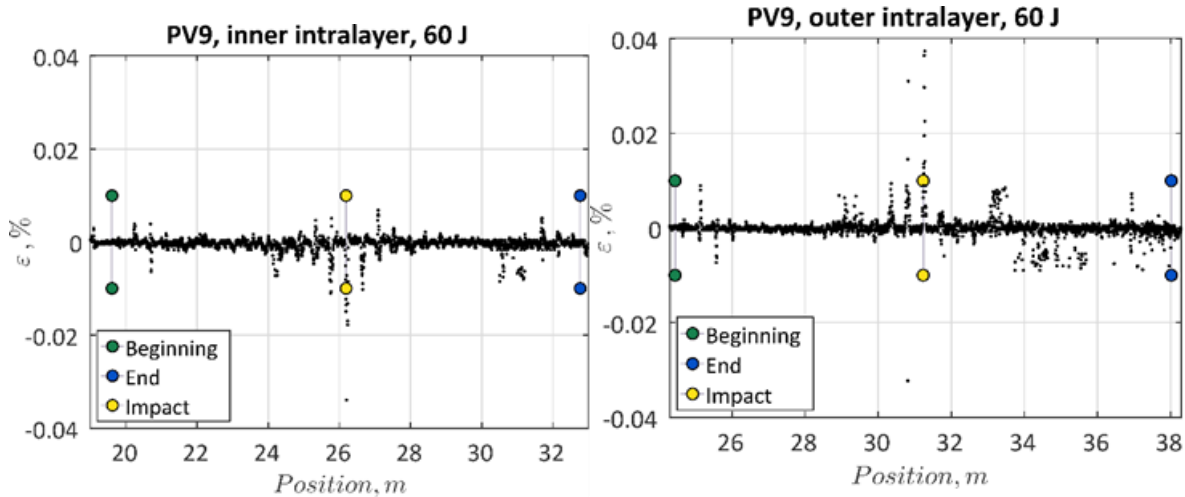

Figure 16: Inner intralayer strains after impact on Vessel 9, with reference markers (Mode 2)

Figure 17: Outer intralayer strains after impact on Vessel 9, with reference markers (Mode 2)

It is obvious that the impact affects a much larger area than what is observed in visual inspection. A typical severe damage on the cylinder surface is shown in Figure 18, consisting of a small imprint from direct impactor contact and fibre fractures in the outermost ply, progressing symmetrically in the axial direction [39]. The visible traces of impacts are very localized, confined to a 30-50 mm region. However, the OFs measure strain peaks from internal delaminations (releasing residual strains), which are visible over almost the entire length of the cylinder.

In Figures 16 and 17 the strains are plotted against the position along the OF length. A network of OFs embedded inside the pressure vessel opens new possibilities for creating detailed visualizations of the damage area. Since the geometry of the vessel is known, the position along the fibre can be decomposed, and plotted on a surface, as seen in Figure 19.

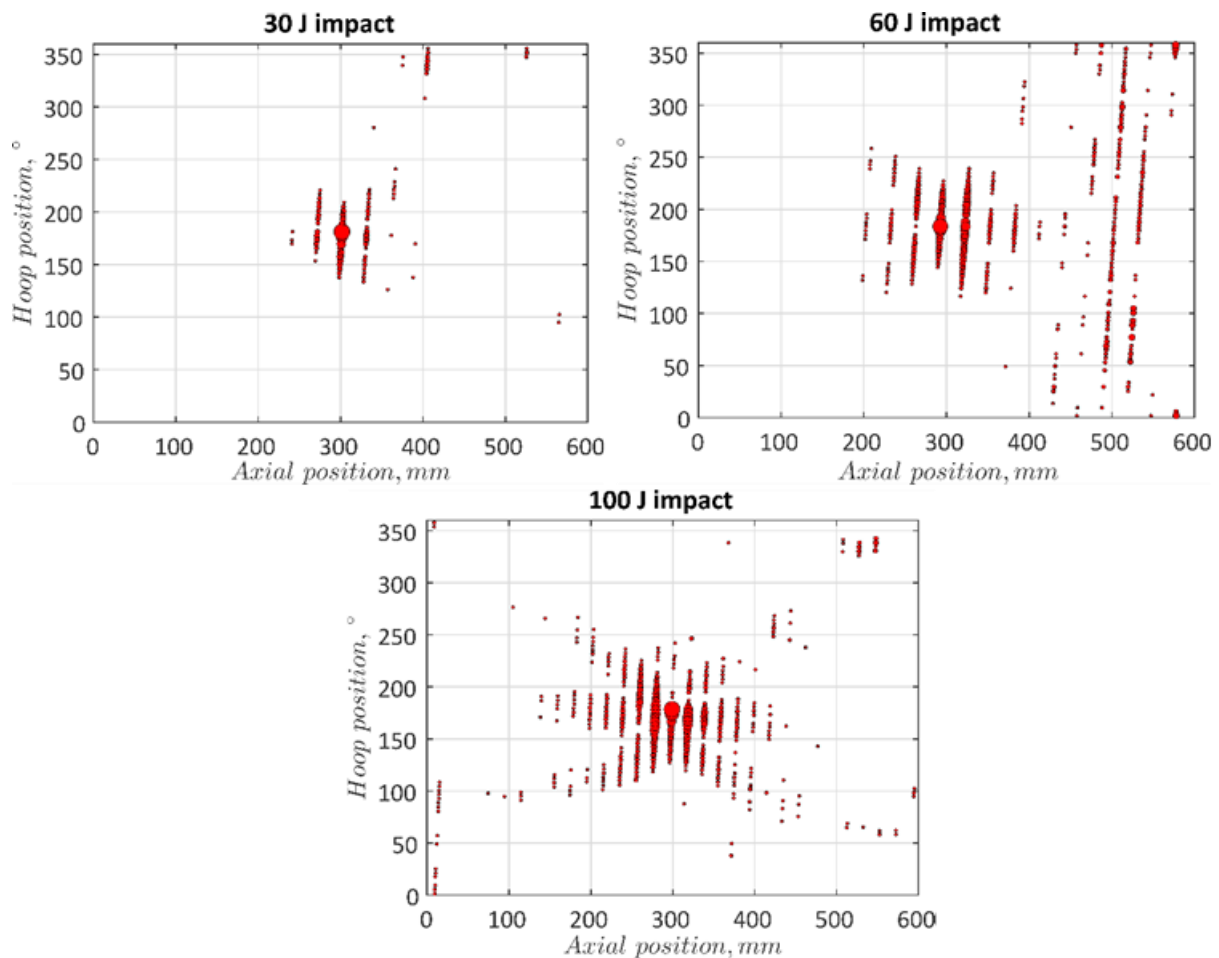*Figure 18: Severe impact damage on the cylinder surface*

Figure 19: Strains measured on unpressurized vessels after impacts on the centre with various energies.

The strains from three pressure vessels, which have been impacted by different impact energies (30 J, 60 J, 100 J) are compared. The strains exceeding the ± 10 microstrain noise threshold are plotted as dots. The diameter of the dots is a logarithmic function of absolute strain values and the same scale was used for all three figures. The impact location near the 300 mm axial coordinate (i.e. in the middle of the pressure vessel) is clearly evident, despite occasional surrounding noise. There is also an obvious correlation between the impact energy applied to the unpressurized vessel, and the overall size of the delaminated region. The higher the applied

energy, the larger the delaminated area. Interestingly, the highest energy impact (100 J) also shows individual bands of delamination, two of which seem to align with ± 15° helical plies.

The importance and the precision of reference points is easy to grasp since this 2-D visualization in Figure 19 relies fully on the knowledge of specific positioning of each individual optical fibre. To obtain a high precision for OF monitoring, it is necessary to have many reference points, even in several intermediate positions along the cylinder length, for longer pressure vessels or tubes.

Strains in optical hoop fibres – pressurized
The previous detection cases were based on non-pressurized vessels. During examination of the pressurization data, evidence of damage could also be revealed by looking at the hoop optical fibres under pressurization. In Figure 20, a strain vs position plot of pressure vessel 2 is shown. The data was already presented in Figure 13, but now all measurement points are connected as a line in the plot. Results for three pressure levels are shown; 20 bar, 70 bar and 120 bar. The highlighted impact is based on the true midpoint of the vessel, where the impact was performed. For the low pressure of 20 bar, the strains are roughly constant. They show small periodic peaks over the centre of the vessel; no indication of damage is present. For the higher pressure levels, the strains around the impact region begin to deviate from the strains seen over the rest of the vessel. For the highest pressure the centre peak grows higher, indicating increasing damage. As seen in Figure 13, the fibre was severed at 160 bar.

The periodic peaks in the roughly constant regions of the strain plots, appearing at both sides of the impact, are spaced by ca. 40-50 cm. This equates to one hoop circumference, which in relation to the optical fibre pitch for PV2, translates to a distance of 30 mm on the vessel surface in the axial direction. It is a secondary effect attributed to initial ovality of the vessel, but it is outside the scope of this paper to investigate this effect in detail. The strain fluctuations in the beginning and end regions are a result of the mandrel configuration, where the steel end domes transition abruptly to a less rigid polyethylene mandrel. The strain peaks caused by impact damage can be easily identified, since they are larger than the periodic peaks and grow with increasing pressure.
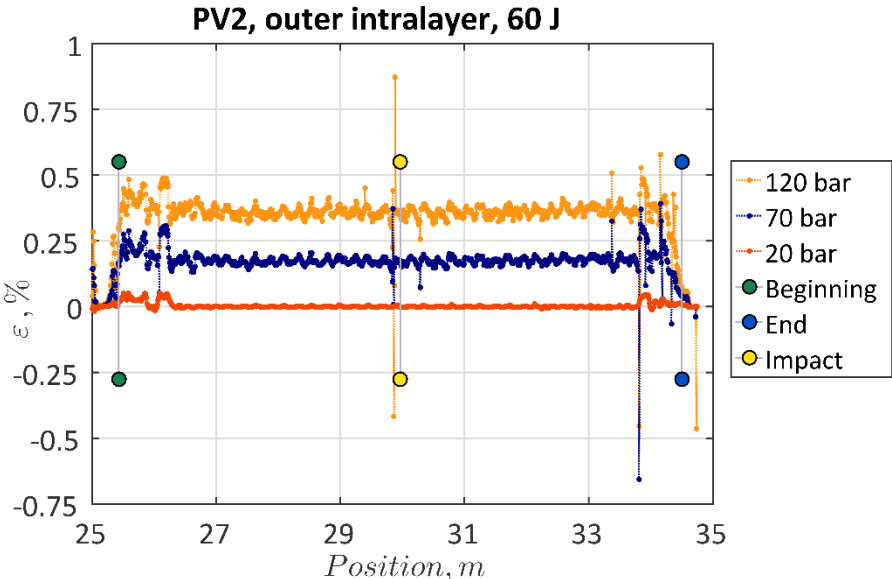

Figure 20: Strains vs position along the optical fibre for three pressure levels, Vessel 2 (Mode 3).

Comparison

The hoop optical fibre configuration is the most promising method for impact detection. The optical fibres are easily embedded into the laminate and damage can be detected on unpressurized and pressurized vessels. Note that the method should also work for surface mounted fibres, but this was not tried in this test program.

The grid method is best for studying the spread of impact damage. The grid is complicated to put into the composite laminate and it works well only if the impact happens in the middle of the grid. This method is good for studying the effect of impact on the vessel, but it is less suited for detecting random impact events.

Fracture of an optical fibre placed close to the surface is an obvious method to detect impact, but it only works if the impact happened close to the fibre. The advantage of using an OBR optical fibre is that the location of the impact is indicated, with high precision.

CONCLUSIONS

- A method is described to monitor for damages due to impacts on filament wound composite pressure vessels. The method is based on using optical fibres (OF) embedded in the laminate, and was successfully demonstrated as a method for structural health monitoring of composite pressure vessels. Four ways of detecting damage were found, where three were used on non-pressurized vessels and one was utilized on pressurized vessels. A novel data analysis method (running reference method) was employed to mitigate noise appearing in the measurements on pressurized vessels.
- The most promising method for detecting the location of an impact event are optical fibres wound continuously in the near hoop direction. A pitch angle of about 2.5-4.0 degrees was used to wind OFs between filaments which themselves had a pitch angles of ±0.7 degrees. The fibres can detect the location of the impact and the spread of damage to some extent. When the pressure vessel is unpressurized the fibres measure the release of residual strains due to the damage. Surface plots were made showing how the damage spreads across the vessel. When the vessel gets pressurized, strain peaks can be seen near the damage.
- The possibility to inspect unpressurized vessels for damage is beneficial from a safety and operational point of view.
- Putting a grid of optical fibres in the vessel allows studying the spread of damage due to impact to the laminate quite accurately, provided the impact hits the centre of the grid. This method is useful for research, but not useful for detecting the location of an unknown impact in a large structure. It is also tedious to apply the grid.
- If the optical fibres get hit directly they fail, and this can also be used as an indication of an impact. This method works best for fibres embedded close to the external surface.
- The embedded optical fibres could measure strains up to the burst pressure of 160 bars. The measured strains were up to 0.5% and compared well with traditional strain measurements from electrical resistance strain gauges. A running reference method was used for the data analysis.
- The embedded optical fibres work best if they are surrounded by structural fibres from the laminate running in about the same direction. The optical fibres worked well and consistent at any through thickness position in the laminate.

ACKNOWLEDGEMENTS

DATA AVAILABILITY

The raw/processed data required to reproduce these findings cannot be shared at this time due to technical and time limitations.

REFERENCES

[1]   Strong AB. Fundamentals of Composites Manufacturing. 2008. doi:10.1016/0956-7143(92)90210-L.

[2]   Lasn K, Vedvik NP, Echtermeyer AT, Blanc-Vannet P, Bardoux O, Alexandre N, et al. Artificial Impact Damage for Estimating the Short-Term Residual Burst Pressure of COPVs. 21st Int. Conf. Compos. Mater., 2017.

[3]   Sansonetti P, M. Leguime D, Engrand P, Ferdinand J, Plantey DH, Bowen, R. Davidson et al. Intelligent Composites Containing Measuring Fibre Optic Networks For Continuous Self Diagnosis. Proc. SPIE 1170, Fiber Opt. Smart Struct. Ski. II, Boston: 1990, p. 211–24. doi:10.1117/12.963099.

[4]   Foedinger RC, Rea DL, Sirkis JS, Baldwin CS, Troll JR, Grande R, et al. Embedded Fiber Optic Sensor Arrays for Structural Health Monitoring of Filament Wound Composite Pressure Vessels. Proc. SPIE 3670, Smart Struct. Mater. 1999 Sens. Phenom. Meas. Instrum. Smart Struct. Mater., Newport Beach, CA: 1999, p. 289–302. doi:10.1117/12.349740.

[5]   Degrieck J, De Waele W. Embedded Optical Fibre Sensors for the Permanent Monitoring of Filament Wound Pressure Vessels. NDT.net, Vol 4, No 3 1999. http://www.ndt.net/article/v04n03/5/5.htm (accessed October 23, 2017).

[6]   Degrieck J, De Waele W, Verleysen P. Monitoring of fibre reinforced composites with embedded optical fibre Bragg sensors, with application to filament wound pressure vessels. NDT E Int 2001;34:289–96. doi:10.1016/S0963-8695(00)00069-4.

[7]   Kang H-K, Park J-S, Kang D-H, Kim C-U, Hong C-S, Kim C-G. Strain monitoring of a filament wound composite tank using fiber Bragg grating sensors. Smart Mater Struct 2002;11:848–53. doi:10.1088/0964-1726/11/6/304.

[8]   Kunzler M, Udd E, Kreger S, Johnson M, Henrie V. Damage Evaluation and Analysis of Composite Pressure Vessels Using Fiber Bragg Gratings to Determine Structural Health. Proc. SPIE 5758, Smart Struct. Mater. 2005 Smart Sens. Technol. Meas. Syst., San Diego, CA: 2005, p. 168–77. doi:10.1117/12.599890.

[9]   Kang DH, Kim CU, Kim CG. The embedment of fiber Bragg grating sensors into filament wound pressure tanks considering multiplexing. NDT E Int 2006;39:109–16. doi:10.1016/j.ndteint.2005.07.013.

[10]   Hao J, Leng J, Wei Z. Non-destructive Evaluation of Composite Pressure Vessel by Using FBG Sensors. Chinese J Aeronaut 2007;20:120–3. doi:10.1016/S1000-9361(07)60017-X.

[11]   Gąsior P, Kaleta J, Sankowska A. Optical Fiber Sensors in Health Monitoring of Composite High-Pressure Vessels for Hydrogen. Proc. SPIE 6616, Opt. Meas. Syst. Ind. Insp. V, 66163G, Munich: 2007. doi:10.1117/12.726111.

[12]   Frias C, Faria H, Frazão O, Vieira P, Marques AT. Manufacturing and testing composite overwrapped pressure vessels with embedded sensors. Mater Des 2010;31:4016–22. doi:10.1016/j.matdes.2010.03.022.

[13]   Glisic B, Inaudi D. Integration of Long-Gage Fiber Optic Sensor into a Fiber-Reinforced Composite Sensing Tape. Proc. SPIE 5050, Smart Struct. Mater. 2003 Smart Sens. Technol. Meas. Syst., San Diego, CA: 2003, p. 179–87. doi:10.1117/12.484262.

[14]   Glisic B, Inaudi D. Health Monitoring of Full Composite CNG Tanks Using Long-Gauge Fiber Optic Sensors. Proc. SPIE 5384, Smart Struct. Mater. 2004 Smart Sens. Technol. Meas. Syst., San Diego, CA: 2004, p. 44–54. doi:10.1117/12.544943.

[15]   Blazejewski W, Czulak A, Gasior P, Kaleta J, Mech R. SMART Composite High Pressure Vessels with Integrated Optical Fiber Sensors. Proc. SPIE 7647, Sensors Smart Struct. Technol. Civil, Mech. Aerosp. Syst. 2010, 764712, San Diego, CA: 2010. doi:10.1117/12.847251.

[16]   Gasior P, Blazejewski W, Kaleta J. Smart Fibre Optic Methods for Structural Health Monitoring of High Pressure Vessels for Hydrogen Storage. Proc. 18th World Hydrog. Energy Conf. 2010 - WHEC 2010 B. 5, 2010, p. 309–14.

[17]   Błażejewski W, Gąsior P, Kaleta J. Application of Optical Fibre Sensors to Measuring the Mechanical Properties of Composite Materials and Structures. In: Attaf B, editor. Adv. Compos. Mater. - Ecodesign Anal., InTech; 2011, p. 221–47. doi:10.5772/13954.

[18]   Hernández-Moreno H, Collombet F, Douchin B, Choqueuse D, Davies P, González Velázquez JL. Entire life time monitoring of filament wound composite cylinders using bragg grating sensors: I. adapted tooling and instrumented specimen. Appl Compos Mater 2009;16:173–82. doi:10.1007/s10443-009-9085-7.

[19]   Hernández-Moreno H, Collombet F, Douchin B, Choqueuse D, Davies P, González Velázquez JL. Entire life time monitoring of filament wound composite cylinders using bragg grating sensors: II. process monitoring. Appl Compos Mater 2009;16:197–209. doi:10.1007/s10443-009-9088-4.

[20]   Hernández-Moreno H, Collombet F, Douchin B, Choqueuse D, Davies P. Entire life time monitoring of filament wound composite cylinders using bragg grating sensors: III. in-service external pressure loading. Appl Compos Mater 2009;16:135–47. doi:10.1007/s10443-009-9082-x.

[21]   Martin AR, Fernando GF, Hale KF. Impact damage detection in filament wound tubes using embedded optical fibre sensors. Smart Mater Struct 1997;6:470–6. doi:10.1088/0964-1726/6/4/012.

[22]   Knapp RH, Robertson IN. A New Concept for Smart Composite Pressure Vessels. Proc. Ninth Int. Offshore Polar Eng. Conf., Brest: 1999, p. 244–48.

[23]   Knapp RH, Robertson IN. Fiber Optic Sensor System for Filament-Wound Pressure Vessels. Proc. Tenth Int. Offshore Polar Eng. Conf., Seattle: 2000, p. 77–82.

[24]   Froggatt M, Moore J. High-spatial-resolution distributed strain measurement in optical fiber with Rayleigh scatter. Appl Opt 1998;37:1735–40. doi:10.1364/AO.37.001735.

[25]   Guemes A, Fernandez-Lopez A, Soller B. Optical fiber distributed sensing - physical principles and applications. Struct Heal Monit 2010;9:233–45. doi:10.1177/1475921710365263.

[26]   Samiec D. Distributed fiber-optic temperature and strain measurement with extremely high spatial resolution. Photonik 2012 2012:10–3.

[27]   Maurin L, Ferdinand P, Nony F, Villalonga S. Ofdr Distributed Strain Measurements for Shm of Hydrostatic Stressed Structures : an Application To High Pressure H 2 Storage Type Iv Composite Vessels – H2E Project. EWSHM - 7th Eur. Work. Struct. Heal. Monit., Nantes: 2014, p. 930–7.

[28]   Klute SM, Metrey DR, Garg N, Rahim NAA. In-Situ Structural Health Monitoring of Composite-Overwrapped Pressure Vessels. SAMPE J 2016;52:7–17.

[29]   Bao X, Chen L. Recent progress in distributed fiber optic sensors. Sensors (Basel) 2012;12:8601–39. doi:10.3390/s120708601.

[30]   Ramakrishnan M, Rajan G, Semenova Y, Farrell G. Overview of Fiber Optic Sensor Technologies for Strain/Temperature Sensing Applications in Composite Materials. Sensors (Basel) 2016;16:99. doi:10.3390/s16010099.

[31]   Luna inc n.d. http://lunainc.com (accessed January 26, 2018).

[32]   Gifford DK. FIBER-OPTICS TEST & MEASUREMENT: Rayleigh Backscatter Reflectometry Boosts Fiber Characterization. LaserFocusWorld 2012.

[33]   Pedrazzani, J. Renee Castellucci M, Sang AK, Froggatt ME, Klute SM, Gifford DK. Fiber Optic Strain Sensing Used to Investigate the Strain Fields in a Wind Turbine Blade and in a Test Coupon with Open Holes. Sampe Tech Conf. Proc., Charleston, SC: 2012.

[34]   Castellucci M, Klute S, Lally EM, Froggatt ME, Lowry D. Three-Axis Distributed Fiber Optic Strain Measurement in 3D Woven Composite Structures. 2013 Smart Struct., San Diego, CA: 2013.

[35]   Grave JHL, Håheim ML, Echtermeyer AT. Measuring changing strain fields in composites with Distributed Fiber-Optic Sensing using the optical backscatter reflectometer. Compos Part B Eng 2015;74:138–46. doi:10.1016/j.compositesb.2015.01.003.

[36]   Grave JHL, Echtermeyer AT. Strain fields in adhesively bonded patch repairs of damaged Metallic beams. Polym Test 2015;48:50–8. doi:10.1016/j.polymertesting.2015.09.013.

[37]   Davidson R, Roberts S. Optical Fiber Sensor Compatibility and Integration with Composite Materials. In: Kelly A, Zweben C, editors. Compr. Compos. Mater., Oxford: Pergamon; 2000, p. 591–606.

[38]   Heinze S, Echtermeyer AT. A Running Reference Analysis Method to Greatly Improve Optical Backscatter Reflectometry Strain Data from the Inside of Hardening and Shrinking Materials. Appl Sci 2018;8:1137. doi:10.3390/app8071137.

[39]   Lasn K, Vedvik NP, Echtermeyer AT. The sensitivity of the burst performance of impact damaged pressure vessels to material strength properties. IOP Conf. Ser. Mater. Sci. Eng., vol. 139, 2016. doi:10.1088/1757-899X/139/1/012029.